HHS Public Access

Author manuscript

Biochem Biophys Res Commun. Author manuscript; available in PMC 2022 January 13.

Published in final edited form as:

Biochem Biophys Res Commun. 2021 June 04; 556: 93–98. doi:10.1016/j.bbrc.2021.03.141.

Protective effects of farnesyltransferase inhibitor on sepsis-induced morphological aberrations of mitochondria in muscle and increased circulating mitochondrial DNA levels in mice

Daisuke Tsuji[a], **Harumasa Nakazawa**[a,*], **Tomoko Yorozu**[a], **Masao Kaneki**[b,c]

[a]Department of Anesthesiology, Kyorin University School of Medicine, Tokyo, Japan

[b]Department of Anesthesia, Critical Care and Pain Medicine, Massachusetts General Hospital, Harvard Medical School, Charlestown, MA, 02129, USA

[c]Shriners Hospitals for Children, Boston, MA, 02114, USA

Abstract

Sepsis remains a leading cause of mortality in critically ill patients and is characterized by multi-organ dysfunction. Mitochondrial damage has been proposed to be involved in the pathophysiology of sepsis. In addition to metabolic impairments resulting from mitochondrial dysfunction, mitochondrial DNA (mtDNA) causes systemic inflammation as a damage-associated molecular pattern when it is released to the circulation. Metabolic derangements in skeletal muscle are a major complication of sepsis and negatively affects clinical outcomes of septic patients. However, limited knowledge is available about sepsis-induced mitochondrial damage in skeletal muscle. Here, we show that sepsis induced profound abnormalities in cristae structure, rupture of the inner and outer membranes and enlargement of the mitochondria in mouse skeletal muscle in a time-dependent manner, which was associated with increased plasma mtDNA levels. Farnesyltransferase inhibitor, FTI-277, prevented sepsis-induced morphological aberrations of the mitochondria, and blocked the increased plasma mtDNA levels along with improved survival. These results indicate that protein farnesylation plays a role in sepsis-induced damage of the mitochondria in mouse skeletal muscle. Our findings suggest that mitochondrial disintegrity in skeletal muscle may contribute to elevated circulating mtDNA levels in sepsis.

Keywords

Sepsis; Mitochondria; Mitochondrial DNA; Farnesyltransferase inhibitor; Skeletal muscle

*Corresponding author. Department of Anesthesiology, Kyorin University School of Medicine, 6-20-2 Sinkawa, Mitaka-city, Tokyo, 181-8611, Japan. hal0413@ks.kyorin-u.ac.jp (H. Nakazawa).

Declaration of competing interest

The authors declare that they have no known competing financial interests or personal relationships that could have appeared to influence the work reported in this paper.

Appendix A. Supplementary data

Supplementary data to this article can be found online at https://doi.org/10.1016/j.bbrc.2021.03.141.

1. Introduction

Sepsis is defined as life-threatening organ dysfunction caused by a dysregulated host response to infection [1] and remains a leading cause of mortality in critically ill patients. Multi-organ dysfunction is a major characteristic of sepsis and has been considered to be a major contributor to mortality of septic patients. However, despite intensive investigation for many years, the pathophysiology of sepsis and the etiology of multi-organ dysfunction remain to be clarified.

Mitochondrial dysfunction/disintegrity is a major complication of sepsis and has been proposed to play an important role in multi-organ dysfunction in sepsis [2,3]. Mitochondrial dysfunction can result in insufficient energy production, impaired cellular metabolism and oxidative stress, which, in turn, lead to dysfunction of cells and organs. Moreover, disruption of mitochondrial integrity induces and/or exacerbates inflammation within the cells and systemically. When the integrity of the organelles is impaired, mitochondrial DNA (mtDNA) is released from the mitochondria to the cytosol and extracellular space. Circulating mtDNA causes systemic inflammatory response by activating toll-like receptor-9 [4,5]. In addition, mtDNA can induce immune suppression [5,6], as well. Thus, mtDNA functions as a damage-associated molecular pattern and is considered to play a role in the pathophysiology of sepsis. Previous studies have shown that circulating mtDNA levels are increased in septic patients [5,7,8], and that elevated circulating mtDNA levels were associated with mortality of septic patients [9,10]. However, it remains unclear how mtDNA is released to the circulation in sepsis.

Mitochondria are compartmentalized by inner and outer membranes. The inner membrane forms invaginations, called cristae, that extend into the matrix. Cristae contain the electron transport chain complexes and ATP synthase [11]. On the other hand, mtDNA is localized in the mitochondrial matrix. Disruption of the membranes leads to leakage of mtDNA, while loss or distortion of cristae structure is associated with decreased capacity of oxidative phosphorylation.

Metabolic derangements in skeletal muscle, including muscle wasting and insulin resistance, are a major complication of sepsis and negatively affects clinical outcomes of septic patients [12]. Recently, we have shown that deficiency of myostatin, a myokine that negatively regulates skeletal muscle mass, not only prevents muscle wasting but also improves survival and bacterial clearance in septic mice [13]. These findings suggest that muscle cachexic changes may not simply be a complication of sepsis, but actually drive development of the disease in mice.

Previous studies showed that sepsis increased mitochondrial area in skeletal muscle in mice [14,15]. On the other hand, an early study reported that sepsis did not significantly alter mitochondrial area in skeletal muscle in baboons [16]. However, the effect of sepsis on cristae structure were not examined in previous studies in mice [14,17]. Nor were time-dependent changes in mitochondrial morphology studied in sepsis.

Protein farnesylation is a posttranslational lipid modification of cysteine residue that is catalyzed by farnesyltransferase. Farnesyltransferase catalyzes the covalent attachment of

farnesyl pyrophosphate to cysteine thiols in the CAAX motif located in the carboxyl terminus, where C represents cysteine, A is any aliphatic acid, and X is any amino acid in the carboxyl terminus. We have shown that farnesyltransferase inhibitor (FTI) improves survival and bacterial clearance in septic mice [18]. In addition, we have shown that FTI prevents burn injury-induced morphological abnormalities of the mitochondria (i.e., enlargement, loss of cristae) in mouse skeletal muscle [19]. Here, we studied the effects of FTI on sepsis-induced alterations in the morphology of the mitochondria and increase in circulating mtDNA levels in mice.

2. Materials and methods

2.1. Animals

All experiments were carried out in accordance with the animal care guidelines of Kyorin University and the study protocol was approved by the University's ethics committee (approval no. 207). Male CD1 mice at 8 weeks of age (Nippon SLC, Shizuoka, Japan) were used in this study. All the mice were housed in a pathogen-free animal housing room with a humidity of 50–60% and temperature of 24–26 °C on a 12-h day/night cycle. Food and water were provided ad libitum.

2.2. Experimental design

Sepsis was induced by cecum ligation and puncture (CLP) as previously described [13,18] with minor modifications. In brief, mice were anesthetized by inhalation of 4% isoflurane and maintained under 1.5–2% isoflurane inhalation. Laparotomy was performed by making a 1.0-cm midline incision in the abdomen to expose the cecum, which was ligated at 1 cm distal to the ileocecal valve using 4–0 silk suture. The ligated cecum was perforated by one through-to-through puncture with 18-gauge needle, and the feces were gently extruded. The abdominal musculature was closed with sutures and followed by closure of the skin with tissue glue. In sham mice, the cecum was fully exposed and then returned to the abdominal cavity, but was neither ligated nor punctured. After the skin closure, prewarmed saline (0.04 ml/kg at 36 °C) was injected subcutaneously in the back. Buprenorphine (0.1 mg/kg, SC) was administered at 30 min prior to the surgery and every 8 h thereafter for 3 days after CLP or sham surgery for analgesia.

To examine time-dependent changes, soleus (slow-twitch) and gastrocnemius (fast-twitch) muscles and blood samples were collected prior to and 24, 48 and 72 h, and 7 and 14 days after CLP under anesthesia with isoflurane.

To evaluate the effects of farnesyltransferase inhibitor (FTI), the mice were treated with FTI-277 (Sigma Aldrich, Tokyo, Japan, cat# F9803) (5 mg/kg/day, SC) or vehicle (saline) every 24 h for 3 days, starting at 2 h after CLP or sham surgery. At 2 h after the final administration of FTI-277 or vehicle, skeletal muscle (soleus and gastrocnemius) and blood samples were collected under anesthesia with isoflurane. At the end of study, the mice were euthanized by carbon dioxide asphyxiation.

2.3. Evaluation of mitochondrial morphology

Mitochondrial morphology was evaluated by transmission electron microscopy as performed in our previous studies [19,20] with minor modifications. Immediately after soleus and gastrocnemius muscles were excised, samples were fixed in a 2.5% paraformaldehyde/2.5% glutaraldehyde solution in 0.1 M sodium cacodylate buffer (pH 7.4) (Electron Microscopy Sciences, Hatfield, PA, cat# 15960–01). Fixed samples were rinsed with PBS and then fixed with 1% osmium tetroxide (Sigma-Aldrich, cat# 75632). Then, the samples were dehydrated in ethanol, then ethanol was replaced with propylene oxide (Fujifilm Wako Pure Chemical Corporation, Osaka, Japan, cat# W01POS00236). After dehydration, the samples were embedded in epoxy resin (Sigma-Aldrich, cat# 45345), and then thin sections (70–80 nm) were prepared and observed under an electron microscope (JEM-1011; JEOL, Tokyo, Japan). 5 fields of view at 2,500× magnification were randomly captured for each sample. Image J software Version1.52 (NIH, Bethesda, MD, USA) was used to perform morphometric analysis of intermyofibrillar mitochondria using the cell counter analysis plugin.

2.4. Measurement of mtDNA levels in plasma

To obtain plasma, heparinized blood samples were centrifuged at 3,000 rpm for 15 min at 4 °C immediately after the blood collection. DNA in plasma was extracted using DNA extraction kit (QIAamp DNA Blood Mini Kit, Qiagen, Tokyo, Japan, cat# 51104). For evaluation of mtDNA levels, cytochrome c oxidase subunit 3 (*COX3*) gene and NADH dehydrogenase subunit 4 (*ND4*) gene were amplified. 5 μl of the diluted sample DNA was amplified in 25 μl of PCR reaction mixture containing SYBR Green Master Mix (Life Technologies, Grand Island, NY, USA, cat# 4309155 and 4306736) and 5 μl of each primer (the final concentration in the reaction mixture: 200 nM). The amplification was evaluated by real-time PCR using Mastercycler (QuantStudio® 5 real-time PCR system, Thermo Fisher Scientific, Fukuoka, Japan). The primers were designed to target *COX3* (Forward: 5′-CGTGAAGGAAACTACCCAGG-3′; Reverse: 3′-CGCTCAGAAGAATCCTGCAA-5′) [21] and *ND4* (Forward: 5′-ATTATTATTACCCGATGAGGGAACC-3′; Reverse: 3′-ATTAAGATGAGGGCAATTAGCAGT-5′) [22] (Sigma-Aldrich).

2.5. Statistical analysis

To analyze the effects of CLP at different time points, the data were compared with one-way ANOVA followed by Bonferroni test for multiple comparison. To analyze the effects of FTI-277 in septic and sham-operated mice, the data were analyzed by two-way ANOVA followed by Bonferroni test for multiple comparison. Log rank test was used to compare survival between the groups in the Kaplan–Meier survival curves. A value of $p < 0.05$ was considered statistically significant. All the data were analyzed by using GraphPad Prism 7.0 and are expressed as means ± SEM.

3. Results

3.1. Sepsis induced morphological aberrations of the mitochondria in skeletal muscle

Transmission electron microscopy revealed that sepsis induced profound morphological abnormalities of the mitochondria in soleus and gastrocnemius muscles, namely partial and complete loss of cristae structure, “onion-like” swirling cristae, rupture of the inner and outer membranes, and enlargement [19,20,23–26] in a time-dependent manner, as compared with naïve mice (Fig. 1 and Supplementary Fig. 1). In naïve mice, over 80% of mitochondrial area was occupied by cristae structure in 92% of the total mitochondria. We classified loss of cristae into 2 categories: (1) partial loss (less than 80% but over 20% of area was occupied by cristae); and (2) complete loss (equal to or less than 20% of area was occupied by cristae) as previously described [25]. Sepsis significantly increased the number of the mitochondria with partial and complete loss of cristae at 1 and 2 days after the induction of sepsis in soleus (Fig. 1D) and at 1, 2, 3 and 7 days after sepsis induction in gastrocnemius (Fig. 1G). The number of the mitochondria with rupture of the membranes was significantly greater in septic mice at 1 and 2 days after sepsis induction in soleus (Fig. 1E) and at 1, 2 and 7 days after sepsis induction in gastrocnemius compared with naïve mice (Fig. 1H). On the other hand, the number of the mitochondria containing swirling cristae was increased at 7 and 14 days after sepsis induction in soleus and gastrocnemius (Fig. 1D and G). In all the mitochondria with swirling cristae, partial loss of cristae was also observed. Densely compacted spots appeared to be increased in the mitochondria in septic mice, but there was no statistical significance (Supplementary Fig. 2). Total mitochondria area and average size of the mitochondria were significantly increased at 1, 2 and/or 3 days after sepsis induction, while the number of the mitochondria was significantly decreased (Fig. 1F and I, Supplementary Fig. 1). Gigantic mitochondria (>1.2 μm^2) were observed in septic, but not naïve, mice (Supplementary Fig.1). Partial or complete loss of cristae was observed in all the gigantic mitochondria, while it was observed in normal size mitochondria, as well.

3.2. Sepsis increased circulating mtDNA levels

mtDNA levels in plasma were evaluated by real-time PCR using primers targeting *COX3* and *ND4* genes. Plasma mtDNA levels were markedly increased in septic mice compared with naïve mice, staring at 1 day after sepsis induction (Fig. 2). At 14 days after sepsis induction, circulating mtDNA levels returned to the basal level observed in naïve mice.

3.3. FTI-277 prevented sepsis-induced morphological aberrations of the mitochondria in skeletal muscle

FTI-277 treatment prevented sepsis-induced morphological alterations of the mitochondria, namely loss of cristae structure, increases in area and size of the mitochondria, and decreased number of the mitochondria in soleus and gastrocnemius muscles at 3 days after sepsis induction, as compared with vehicle alone (Fig. 3 and Supplementary Fig. 3). On the other hand, FTI-277 did not induce morphological alterations in sham mice. Neither sepsis nor FTI-277 significantly altered the number of the mitochondria with swirling cristae or densely compacted spots at 3 days after sepsis induction (Fig. 3 and Supplementary Fig. 4).

3.4. FTI-277 prevented sepsis-induced increase in circulating mtDNA levels

Real-time PCR for *COX-3* and *ND4* genes revealed that FTI-277 treatment blocked sepsis-induced increase in plasma mtDNA levels at 3 days after sepsis induction compared with vehicle alone (Fig. 4A and B). Consistent with our previous study [18], FTI-277 significantly improved survival of septic mice (Fig. 4C).

4. Discussion

Here, we show that sepsis induced profound time-dependent morphological aberrations of the mitochondria in skeletal muscle and marked increase in circulating mtDNA levels in mice and that FTI-277 treatment prevented these alterations in septic mice.

Sepsis caused loss of cristae, rupture of the outer and inner membranes and emergence of markedly enlarged mitochondria in mouse skeletal muscle starting at 1 day after sepsis induction. The maximum effects of sepsis on these morphological abnormalities were observed at 1 and/or 2 days after sepsis induction. Since the electron transport chain complexes and ATP synthase reside in cristae [27], one can reasonably speculate that loss of cristae may be associated with impaired function of the electron transport chain, namely decreased capacity of oxidative phosphorylation and increased reactive oxygen generation by the electron transport chain. In addition, rupture of the inner and outer membranes results in leakage of mtDNA from the mitochondria. Skeletal muscle is the largest organ in the body and constitutes 30–40% of body weight in healthy adults [28]. It is, therefore, conceivable that the membrane rupture of the mitochondria in skeletal muscle may contribute to increased circulating mtDNA in sepsis. On the other hand, the mitochondria containing “onion-like” swirling cristae increased in number at 7 and 14 days after sepsis induction, but not in the early stage of sepsis. Of note, swirling cristae was accompanied by partial loss of cristae in these mitochondria. The emergence of swirling cristae at the late stage of sepsis is consistent with a previous study in which mitochondrial morphology was examined at 2 weeks after sepsis induction [25], although they did not study time-dependent changes. It is reasonable to speculate that swirling cristae may appear in the recovery phase from mitochondrial damage. However, the biological implication of swirling cristae is not known.

FTI-277 blocked sepsis-induced morphological aberrations of the mitochondria (i.e., loss of cristae, enlargement), which paralleled reversal of elevated circulating mtDNA levels and reduced mortality rate in septic mice. These results are in line with our previous studies on the effects of FTI-277 in septic mice [18] and burned mice [19]. We have shown that FTI-277: (1) improved survival of septic mice [18]; and (2) prevented burn injury-induced mitochondrial dysfunction/disintegrity in mouse skeletal muscle [19]. Our data suggest that protein farnesylation may play an important role in disruption of mitochondrial integrity in skeletal muscle in septic mice.

Supplementary Material

Refer to Web version on PubMed Central for supplementary material.

Acknowledgements

We thank Ms. Y. Matsubara and Prof. Y. Akiyama (Department of Anatomy, Kyorin University School of Medicine) for their technical assistance on electron microscopy.

Funding

This work was supported by research grants to HN from JSPS KAKENHI (17K18084 and 20K09273), to DT from JSPS KAKENHI (20K17727) and to MK from the National Institutes of Health (NIH; R01GM115552, R01GM117298). The funders had no role in study design, data collection and analysis, decision to publish, or preparation of the manuscript.

References

[1]. Singer M, Deutschman CS, Seymour CW, Shankar-Hari M, Annane D, Bauer M, Bellomo R, Bernard GR, Chiche JD, Coopersmith CM, Hotchkiss RS, Levy MM, Marshall JC, Martin GS, Opal SM, Rubenfeld GD, van der Poll T, Vincent JL, Angus DC, The third international consensus definitions for sepsis and septic shock (Sepsis-3), J. Am. Med. Assoc. 315 (2016) 801–810.

[2]. Exline MC, Crouser ED, Mitochondrial mechanisms of sepsis-induced organ failure, Front. Biosci. 13 (2008) 5030–5041. [PubMed: 18508567]

[3]. Arulkumaran N, Deutschman CS, Pinsky MR, Zuckerbraun B, Schumacker PT, Gomez H, Gomez A, Murray P, Kellum JA, Workgroup AX, Mitochondrial function in sepsis, Shock 45 (2016) 271–281. [PubMed: 26871665]

[4]. Zhang Q, Raoof M, Chen Y, Sumi Y, Sursal T, Junger W, Brohi K, Itagaki K, Hauser CJ, Circulating mitochondrial DAMPs cause inflammatory responses to injury, Nature 464 (2010) 104–107. [PubMed: 20203610]

[5]. Schafer ST, Franken L, Adamzik M, Schumak B, Scherag A, Engler A, Schonborn N, Walden J, Koch S, Baba HA, Steinmann J, Westendorf AM, Fandrey J, Bieber T, Kurts C, Frede S, Peters J, Limmer A, Mitochondrial DNA: an endogenous trigger for immune paralysis, Anesthesiology 124 (2016) 923–933. [PubMed: 26808636]

[6]. Konecna B, Park J, Kwon WY, Vlkova B, Zhang Q, Huang W, Kim HI, Yaffe MB, Otterbein LE, Itagaki K, Hauser CJ, Monocyte exocytosis of mitochondrial danger-associated molecular patterns in sepsis suppresses neutrophil chemotaxis, J Trauma Acute Care Surg 90 (2021) 46–53. [PubMed: 33021603]

[7]. Faust HE, Reilly JP, Anderson BJ, Ittner CAG, Forker CM, Zhang P, Weaver BA, Holena DN, Lanken PN, Christie JD, Meyer NJ, Mangalmurti NS, Shashaty MGS, Plasma mitochondrial DNA levels are associated with ARDS in trauma and sepsis patients, Chest 157 (2020) 67–76. [PubMed: 31622590]

[8]. Di Caro V, Walko TD 3rd, Bola RA, Hong JD, Pang D, Hsue V, Au AK, Halstead ES, Carcillo JA, Clark RS, Aneja RK, Plasma mitochondrial DNA–a novel DAMP in pediatric sepsis, Shock 45 (2016) 506–511. [PubMed: 26682947]

[9]. Yang Y, Yang J, Yu B, Li L, Luo L, Wu F, Wu B, Association between circulating mononuclear cell mitochondrial DNA copy number and in-hospital mortality in septic patients: a prospective observational study based on the Sepsis-3 definition, PloS One 14 (2019), e0212808.

[10]. Wang L, Zhou W, Wang K, He S, Chen Y, Predictive value of circulating plasma mitochondrial DNA for Sepsis in the emergency department: observational study based on the Sepsis-3 definition, BMC Emerg. Med. 20 (2020) 25. [PubMed: 32299369]

[11]. Beger HG, Mayer B, Rau BM, Parenchyma-sparing, limited pancreatic head resection for benign tumors and low-risk periampullary cancer–a systematic review, J. Gastrointest. Surg. 20 (2016) 206–217. [PubMed: 26525207]

[12]. Kaneki M, Metabolic inflammatory complex in sepsis: septic cachexia asa novel potential therapeutic target, Shock 48 (2017) 600–609. [PubMed: 28520694]

[13]. Kobayashi M, Kasamatsu S, Shinozaki S, Yasuhara S, Kaneki M, Myostatin deficiency not only prevents muscle wasting but also improves survival in septic mice, Am. J. Physiol. Endocrinol. Metab. 320 (2021) E150–E159. [PubMed: 33284091]

[14]. Bloise FF, Santos AT, de Brito J, de Andrade CBV, Oliveira TS, de Souza AFP, Fontes KN, Silva JD, Blanco N, Silva PL, Rocco PRM, Fliers E, Boelen A, da-Silva WS, Ortiga-Carvalho TM, Sepsis impairs thyroid hormone signaling and mitochondrial function in the mouse diaphragm, Thyroid 30 (2020) 1079–1090. [PubMed: 32200709]

[15]. Leduc-Gaudet JP, Mayaki D, Reynaud O, Broering FE, Chaffer TJ, Hussain SNA, Gouspillou G, Parkin overexpression attenuates sepsisinduced muscle wasting, Cells (2020) 9.

[16]. Welty-Wolf KE, Simonson SG, Huang YC, Fracica PJ, Patterson JW, Piantadosi CA, Ultrastructural changes in skeletal muscle mitochondria in gram-negative sepsis, Shock 5 (1996) 378–384. [PubMed: 9156795]

[17]. Boicelli A, Caramelli E, Baldassarri AM, Giuliani AM, Capitani S, Billi AM, Manzoli FA, 1H-NMR relaxation study of the liposome–nuclei interaction, Physiol. Chem. Phys. Med. NMR 20 (1988) 273–279. [PubMed: 3254538]

[18]. Yang W, Yamada M, Tamura Y, Chang K, Mao J, Zou L, Feng Y, Kida K, Scherrer-Crosbie M, Chao W, Ichinose F, Yu YM, Fischman AJ, Tompkins RG, Yao S, Kaneki M, Farnesyltransferase inhibitor FTI-277 reducesmortality of septic mice along with improved bacterial clearance, J. Pharmacol. Exp. Therapeut. 339 (2011) 832–841.

[19]. Nakazawa H, Ikeda K, Shinozaki S, Kobayashi M, Ikegami Y, Fu M, Nakamura T, Yasuhara S, Yu YM, Martyn JAJ, Tompkins RG, Shimokado K, Yorozu T, Ito H, Inoue S, Kaneki M, Burn-induced muscle metabolic derangements and mitochondrial dysfunction are associated with activation of HIF-1alpha and mTORC1: role of protein farnesylation, Sci. Rep. 7 (2017) 6618. [PubMed: 28747716]

[20]. Nakazawa H, Ikeda K, Shinozaki S, Yasuhara S, Yu YM, Martyn JAJ, Tompkins RG, Yorozu T, Inoue S, Kaneki M, Coenzyme Q10 protects against burn-induced mitochondrial dysfunction and impaired insulin signaling in mouse skeletal muscle, FEBS Open Bio 9 (2019) 348–363.

[21]. Tsuji N, Tsuji T, Ohashi N, Kato A, Fujigaki Y, Yasuda H, Role of mitochondrial DNA in septic AKI via toll-like receptor 9, J. Am. Soc. Nephrol. 27 (2016) 2009–2020. [PubMed: 26574043]

[22]. Gubina NE, Merekina OS, Ushakova TE, Mitochondrial DNA transcription in mouse liver, skeletal muscle, and brain following lethal x-ray irradiation, Biochemistry (Mosc.) 75 (2010) 777–783. [PubMed: 20636270]

[23]. Jang JY, Blum A, Liu J, Finkel T, The role of mitochondria in aging, J. Clin. Invest. 128 (2018) 3662–3670. [PubMed: 30059016]

[24]. Jiang YF, Lin SS, Chen JM, Tsai HZ, Hsieh TS, Fu CY, Electron tomographic analysis reveals ultrastructural features of mitochondrial cristae architecture which reflect energetic state and aging, Sci. Rep. 7 (2017) 45474. [PubMed: 28358017]

[25]. Owen AM, Patel SP, Smith JD, Balasuriya BK, Mori SF, Hawk GS, Stromberg AJ, Kuriyama N, Kaneki M, Rabchevsky AG, Butterfield TA, Esser KA, Peterson CA, Starr ME, Saito H, Chronic muscle weakness and mitochondrial dysfunction in the absence of sustained atrophy in a preclinical sepsis model, Elife 8 (2019).

[26]. Walker DW, Benzer S, Mitochondrial “swirls” induced by oxygen stress and in the Drosophila mutant hyperswirl, Proc. Natl. Acad. Sci. U. S. A. 101 (2004) 10290–10295. [PubMed: 15229323]

[27]. Kuhlbrandt W, Structure and function of mitochondrial membrane protein complexes, BMC Biol. 13 (2015) 89. [PubMed: 26515107]

[28]. Janssen I, Heymsfield SB, Wang ZM, Ross R, Skeletal muscle mass and distribution in 468 men and women aged 18–88 yr, J. Appl. Physiol. 89 (2000) 81–88. [PubMed: 10904038]

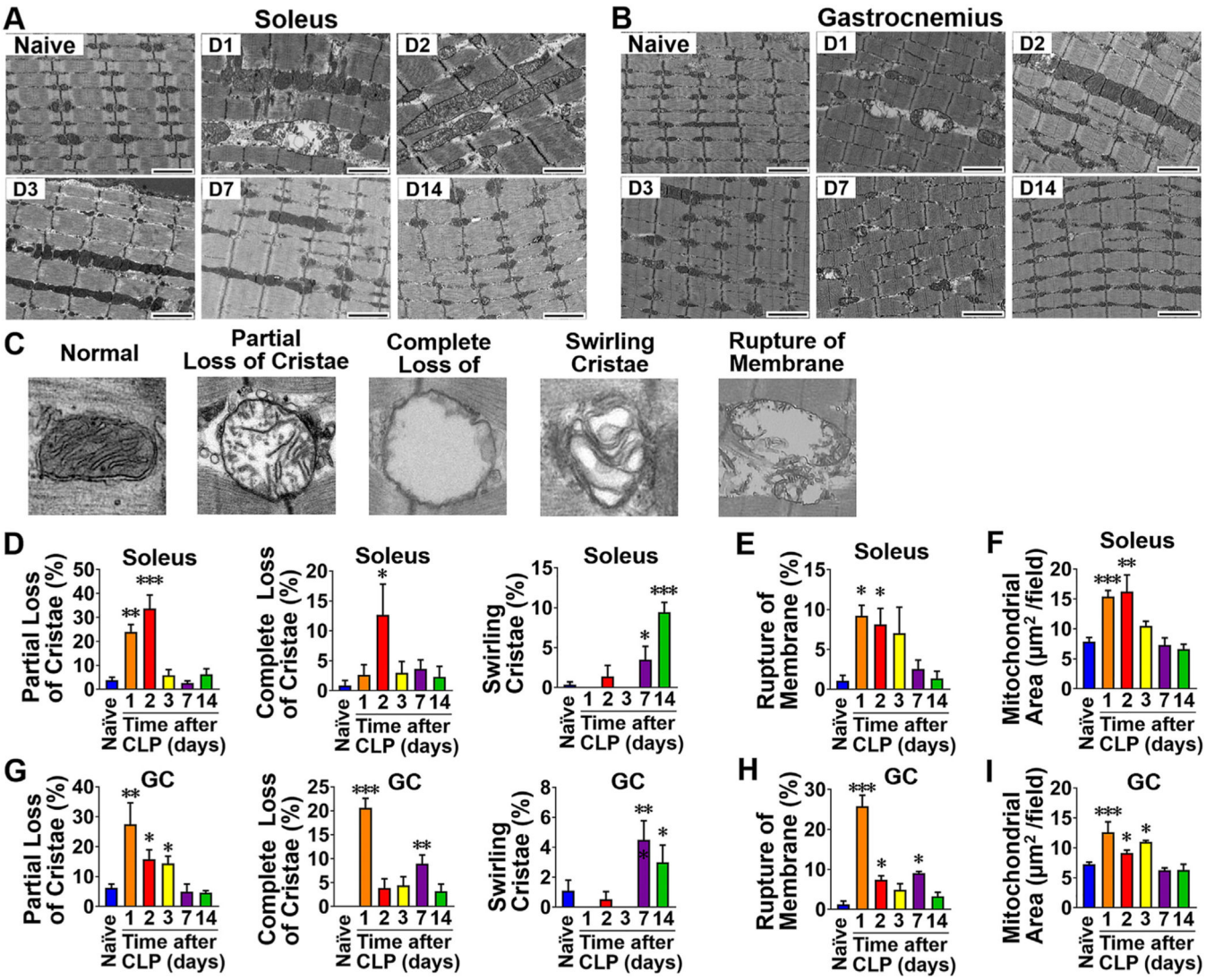

Fig. 1.

Sepsis induced morphological aberrations of the mitochondria in mouse skeletal muscle. (A, B) Representative micrographs of the mitochondria in soleus (A) and gastrocnemius (B) at 2,500× magnification. Scale bar: 2 μm. (C) Representative images of the mitochondria with normal and aberrant morphology. (D–I) Sepsis increased the numbers of the mitochondria with partial and complete loss of cristae or swirling cristae (D, G) and those with rupture of the inner and outer membranes (E, H), and area of the mitochondria (F, I) in soleus (D–F) and gastrocnemius (G–I). CLP: cecum ligation and puncture, GC: gastrocnemius. *$p < 0.05$, **$p < 0.01$, ***$p < 0.001$ vs. naïve mice, n = 5 per group.

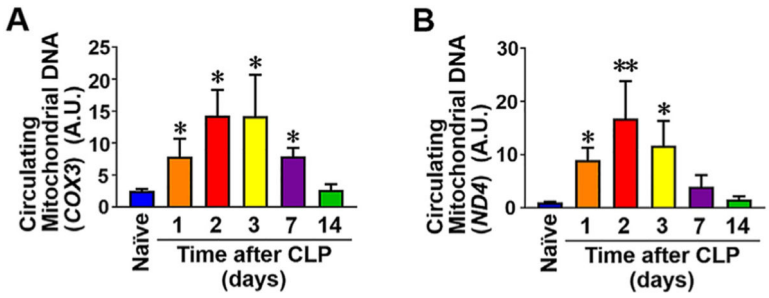

Fig. 2.

Sepsis increased circulating mitochondrial DNA levels. Real-time PCR using primers targeting *COX3* (A) and *ND4* genes (B) showed significantly increased plasma mtDNA levels in septic mice compared with naïve mice. CLP: cecum ligation and puncture. $p < 0.05$, $^{**}p < 0.01$ vs. naïve mice. n = 6 per group.

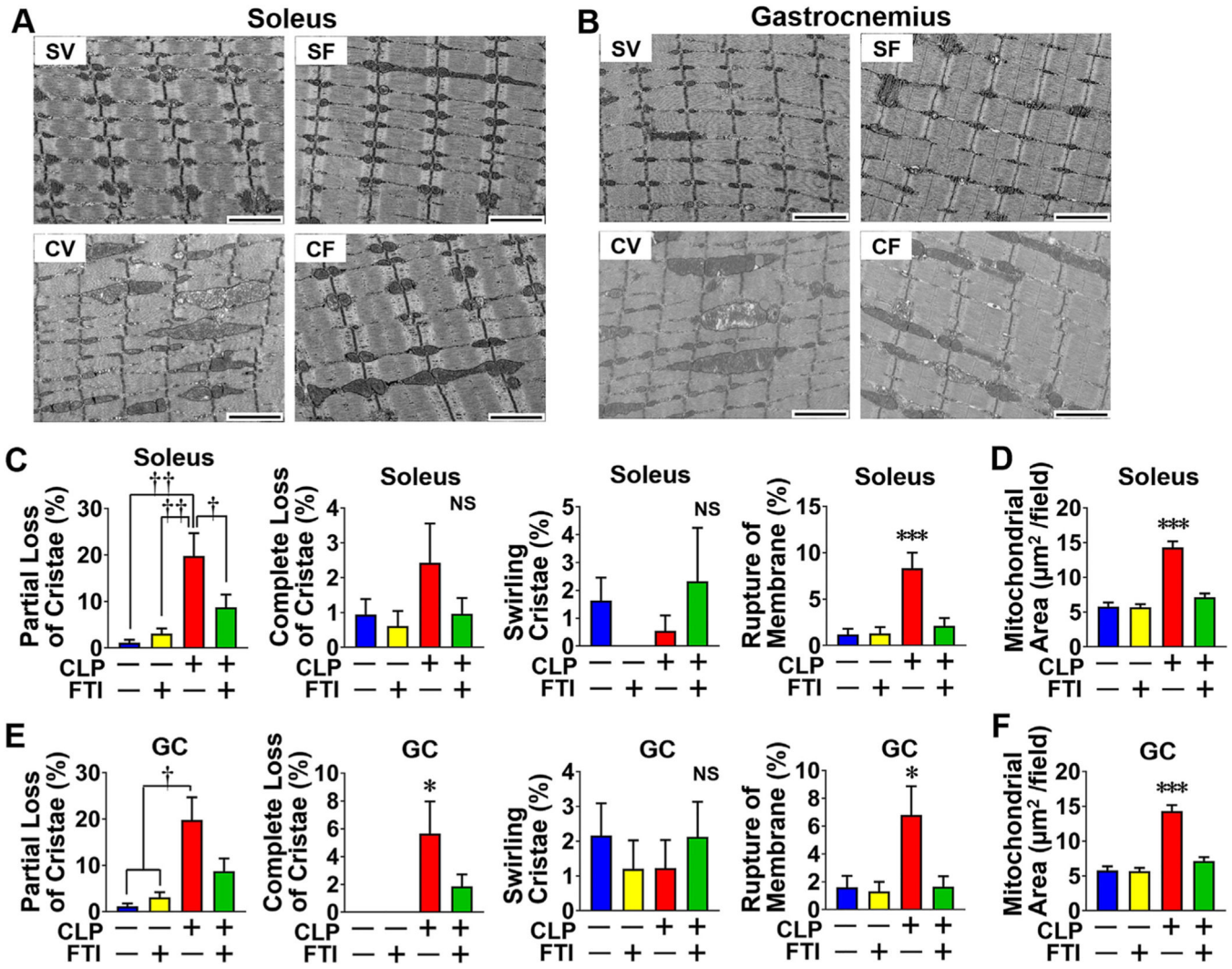

Fig. 3.

FTI-277 treatment prevented sepsis-induced morphological aberrations of the mitochondria in mouse skeletal muscle. FTI-277 treatment inhibited sepsis-induced loss of cristae and increases in rupture of the inner and outer membranes, and increase in mitochondrial area in soleus (A, D-F) and gastrocnemius (B, G-I) at 3 days after sepsis induction by cecum ligation and puncture (CLP). FTI-277 did not induce morphological changes of the mitochondria in sham mice. GC: gastrocnemius, SV: vehicle-treated sham mice, SF: FTI-277-treated sham mice, CV: vehicle-treated CLP mice, CF: FTI-277-treated CLP mice. *p < 0.05, **p < 0.01, ***p < 0.001 vs. SV, SF and CF, n = 6-8 per group.

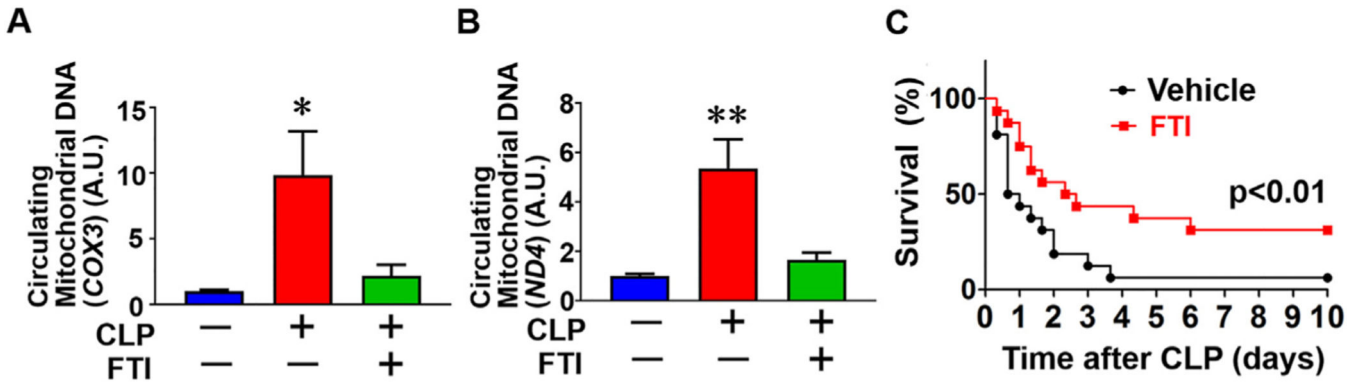

Fig. 4.

FTI-277 treatment inhibited sepsis-induced increase in circulating mtDNA levels and improved survival of septic mice. (A, B) FTI-277 treatment prevented sepsis-induced increased mtDNA levels in plasma, as judged by real-time PCR using primers targeting *COX3* (A) and *ND4* (B) genes. *p < 0.05, **p < 0.01. n = 6 per group. (C) FTI-277 improved survival of septic mice. n = 16 per group. CLP: cecum ligation and puncture.